Article
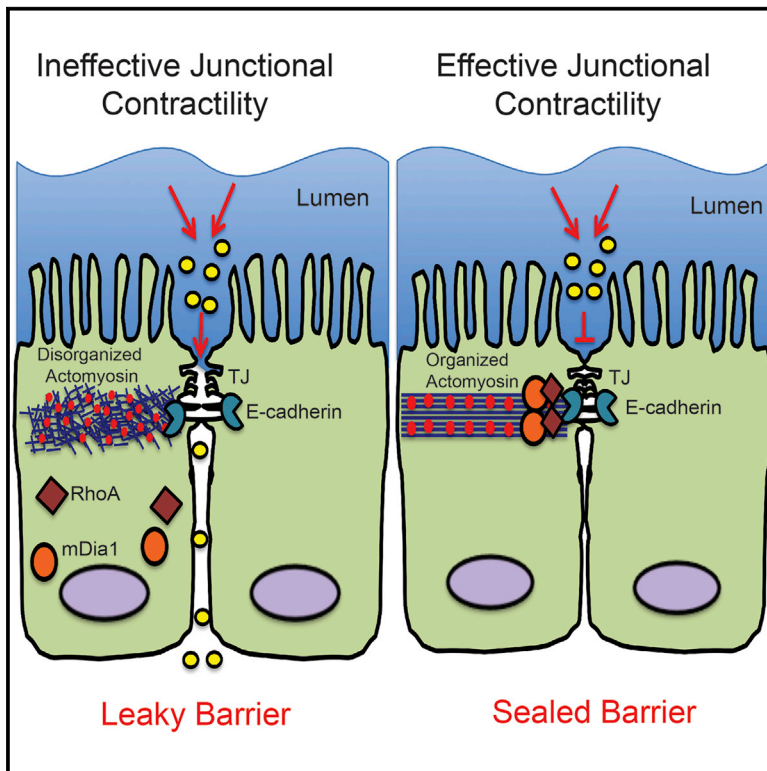
Mammalian Diaphanous 1 Mediates a Pathway for E-cadherin to Stabilize Epithelial Barriers through Junctional Contractility

Graphical Abstract

Authors
Bipul R. Acharya, Selwin K. Wu,
Zi Zhao Lieu, ..., Alexander D. Bershadsky,
Guillermo A. Gomez, Alpha S. Yap

Correspondence
a.yap@uq.edu.au

In Brief
Adherens junctions are contractile structures. Acharya et al. find that the formin mDia1 regulates F-actin organization for effective contractility. mDia1-dependent junctional tension also stabilized components of the tight junction to regulate transepithelial permeability, suggesting that junctional contractility is an element that supports the essential barrier function of post-morphogenetic epithelia.

Highlights

- mDia1 is recruited to the zonula adherens by E-cadherin adhesion and RhoA

- mDia1 supports junctional tension, measured by an αE-catenin tension sensor

- mDia1 reorganizes F-actin to stabilize actomyosin at the ZA

- mDia1-based contractility stabilizes tight junctions and the epithelial barrier

CrossMark

CellPress

Mammalian Diaphanous 1 Mediates a Pathway for E-cadherin to Stabilize Epithelial Barriers through Junctional Contractility

Bipul R. Acharya,[1] Selwin K. Wu,[1] Zi Zhao Lieu,[3] Robert G. Parton,[1,2] Stephan W. Grill,[4,5] Alexander D. Bershadsky,[3] Guillermo A. Gomez,[1] and Alpha S. Yap[1,6,*]

[1]Division of Cell Biology and Molecular Medicine, Institute for Molecular Bioscience, The University of Queensland St. Lucia, Brisbane, QLD 4072, Australia
[2]Centre for Microscopy and Microanalysis, The University of Queensland St. Lucia, Brisbane, QLD 4072, Australia
[3]Mechanobiology Institute of Singapore, National University of Singapore, Singapore 117411, Singapore
[4]Biotechnology Center, Technical University Dresden, Tatzberg 47/49, 01307 Dresden, Germany
[5]Max Planck Institute of Molecular Cell Biology and Genetics, Pfotenhauerstrasse 108, 01307 Dresden, Germany
[6]Lead Contact
*Correspondence: a.yap@uq.edu.au
http://dx.doi.org/10.1016/j.celrep.2017.02.078

SUMMARY

Formins are a diverse class of actin regulators that influence filament dynamics and organization. Several formins have been identified at epithelial adherens junctions, but their functional impact remains incompletely understood. Here, we tested the hypothesis that formins might affect epithelial interactions through junctional contractility. We focused on mDia1, which was recruited to the zonula adherens (ZA) of established Caco-2 monolayers in response to E-cadherin and RhoA. mDia1 was necessary for contractility at the ZA, measured by assays that include a FRET-based sensor that reports molecular-level tension across αE-catenin. This reflected a role in reorganizing F-actin networks to form stable bundles that resisted myosin-induced stress. Finally, we found that the impact of mDia1 ramified beyond adherens junctions to stabilize tight junctions and maintain the epithelial permeability barrier. Therefore, control of tissue barrier function constitutes a pathway for cadherin-based contractility to contribute to the physiology of established epithelia.

INTRODUCTION

Cell-cell junctions couple epithelial individual cells together to form coherent populations. They are necessary for morphogenesis and allow epithelia to form effective tissue barriers. Specialized epithelial junctions serve distinct functions: E-cadherin-based adherens junctions (AJs) promote cell-cell adhesion (Takeichi, 2014), whereas tight junctions (TJs) seal the intercellular space (Marchiando et al., 2010; Anderson and Van Itallie, 2009). AJs and TJs are also dynamic structures, whose morphologies alter, and molecular constituents turn over, in response to physiological and pathological stimuli (Takeichi, 2014; March-

iando et al., 2010; Shen et al., 2008). Recent advances have identified cellular contractility as an important determinant of junctional function (Lecuit and Yap, 2015; Priya et al., 2013; Marchiando et al., 2010). AJs, in particular, are active mechanical structures that display contractile tension (Lecuit and Yap, 2015). This is best understood to function during morphogenesis (Mason et al., 2016; Martin and Goldstein, 2014), but tension is also found at AJs in stable monolayers that are not undergoing morphogenetic movements (Kannan and Tang, 2015; Ratheesh et al., 2012). What role this post-morphogenetic contractility plays in epithelial biology, however, is less well understood.

Contractile tension at AJs is generated by an actomyosin cortex that couples to E-cadherin adhesions (Lecuit and Yap, 2015). This is especially evident in cells that form a zonula adherens (ZA), a site of high junctional tension in polarized simple epithelia (Wu et al., 2014), where prominent actomyosin bundles run adjacent to a ring of stabilized E-cadherin (Wu et al., 2014; Priya et al., 2013; Kovacs et al., 2011; Smutny et al., 2010). These actomyosin bundles are dynamic structures (Michael et al., 2016; Kovacs et al., 2011; Yamada et al., 2005) sustained by an ensemble of molecular processes, many of which are recruited to the junctional cortex in response to E-cadherin (Lecuit and Yap, 2015). These include RhoA signaling, which activates non-muscle myosin (NMII) (Priya and Yap, 2015; Ratheesh et al., 2012). In addition, molecules that control the assembly and organization of junctional F-actin networks are important for effective contractile tension (Jodoin et al., 2015; Kovacs et al., 2011). Not only is junctional actin assembly necessary to sustain F-actin content (Verma et al., 2012), but it also incorporates a process of architectural reorganization that converts disorganized nascent networks into the bundles seen at the mature ZA (Michael et al., 2016). We found that architectural reorganization was necessary to generate effective contractility and identified Coronin 1B as one element of its cellular apparatus (Michael et al., 2016), although it is unlikely to be the only one.

Formins are a large class of actin-binding proteins that are implicated in generating parallel F-actin networks (Goode and Eck, 2007). Biochemically, formins nucleate and elongate

CrossMark
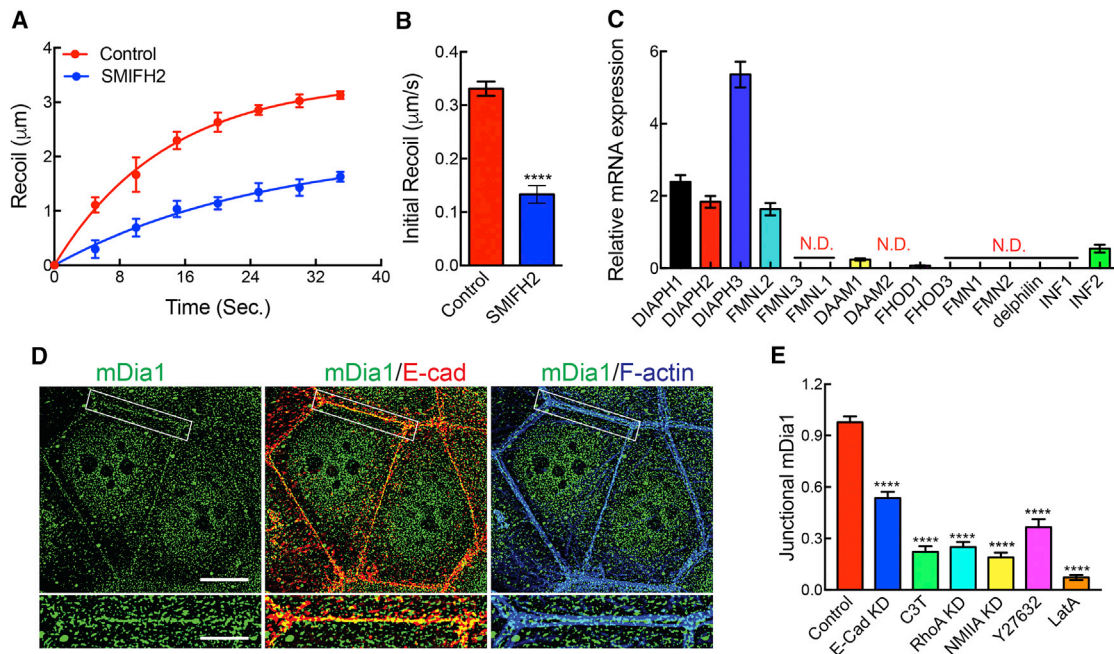
Figure 1. Human mDia1 Concentrates at the Zonula Adherens of Caco-2 Cells
(A and B) Effect of SMIFH2 (50 μM) on vertex recoil (A) and initial recoil velocity (B) of E-Cad-GFP junctions following laser ablation (20–25 junctions/condition/experiment; n = 3 independent experiments); see also Movie S1.
(C) Expression of human formin mRNA in Caco-2 cells relative to GAPDH.
(D) mDia1, F-actin, and E-cadherin immunostaining at the apical ZA imaged by structured illumination microscopy (SIM). Scale bars, 10 and 2 μm (cropped region).
(E) Determinants of mDia1 localization at the ZA. Fluorescence intensity data were normalized to the untreated control.
Data are means ± SEM from n = 3 independent experiments. ****p < 0.0001; unpaired t test with Welch's correction (B) or one-way ANOVA with Dunnett's post hoc test (E). See also Figure S1 and Table S1.

unbranched actin filaments and can also bundle filaments. Several formins have already been identified at AJs, all of which contribute to generating an actin-rich cortex and support AJ integrity (Rao and Zaidel-Bar, 2016; Grikscheit et al., 2015; Mason et al., 2013; Homem and Peifer, 2008; Carramusa et al., 2007; Kobielak et al., 2004). Despite this, the processes that link these phenomena remain poorly understood. In this study, we considered the hypothesis that formins might influence cell-cell interactions by regulating junctional contractility. We tested this by utilizing fluorescence resonance energy transfer (FRET)-based tension sensor (TS) technology (Grashoff et al., 2010) to develop a probe for molecular-level tension across αE-catenin. We identify mammalian Diaphanous 1 (mDia1) at the ZA of human Caco-2 colon epithelial cells and show that it participates in the actin architectural reorganization necessary for junctional tension. We further find that epithelial permeability and TJ stability are compromised in mDia1-deficient cells. This implies that contractility established at the ZA may play a key role in determining how epithelia perform their physiological function as tissue barriers in the body.

RESULTS

### Formin Activity Supports Junctional Tension at the Zonula Adherens
As a first step, we treated confluent Caco-2 human colon epithelial monolayers with the formin inhibitor, SMIFH2 (50 μM; Rizvi

et al., 2009) and tested its effect on junctional tension as measured by laser ablation. Caco-2 cells assemble prominent, E-cadherin-enriched ZAs at their apical-lateral interfaces (Wu et al., 2014; Meng et al., 2008) (Figure S1A). We used cells where E-cadherin-GFP was reconstituted on an E-cadherin small hairpin RNA (shRNA) (knockdown [KD]) background and monitored the instantaneous recoil of vertices after ZA were cut as a measure of the pre-existing tension (Ratheesh et al., 2012). Although SMIFH2 decreased the amount of E-cadherin found at apical junctions (Figure S1A), we were readily able to track recoil of vertices (Movie S1). SMIFH2 reduced junctional recoil (Figures 1A and 1B) without any evident change in frictional drag as reflected in rate constants (k-values) for relaxation of junctions (Table S1). Together, these suggested that the observed differences in recoil velocity principally reflected differences in contractile tension.

mDia1 Is a Candidate Formin to Regulate Tension at the ZA
Fifteen formins are found in the human genome, whose expression varies. Semiquantitative RT-PCR showed that *DIAPH1*, *DIAPH2*, *DIAPH3*, and *FMNL2* had the highest mRNA expression in our Caco-2 cells (Figure 1C). Immunofluorescence analysis revealed that human mDia1 and mDia2 (the protein products of human *Diaph1* and *Diaph2*, respectively) co-accumulated with E-cadherin at the ZA (Figure S1B), whereas human mDia3 and
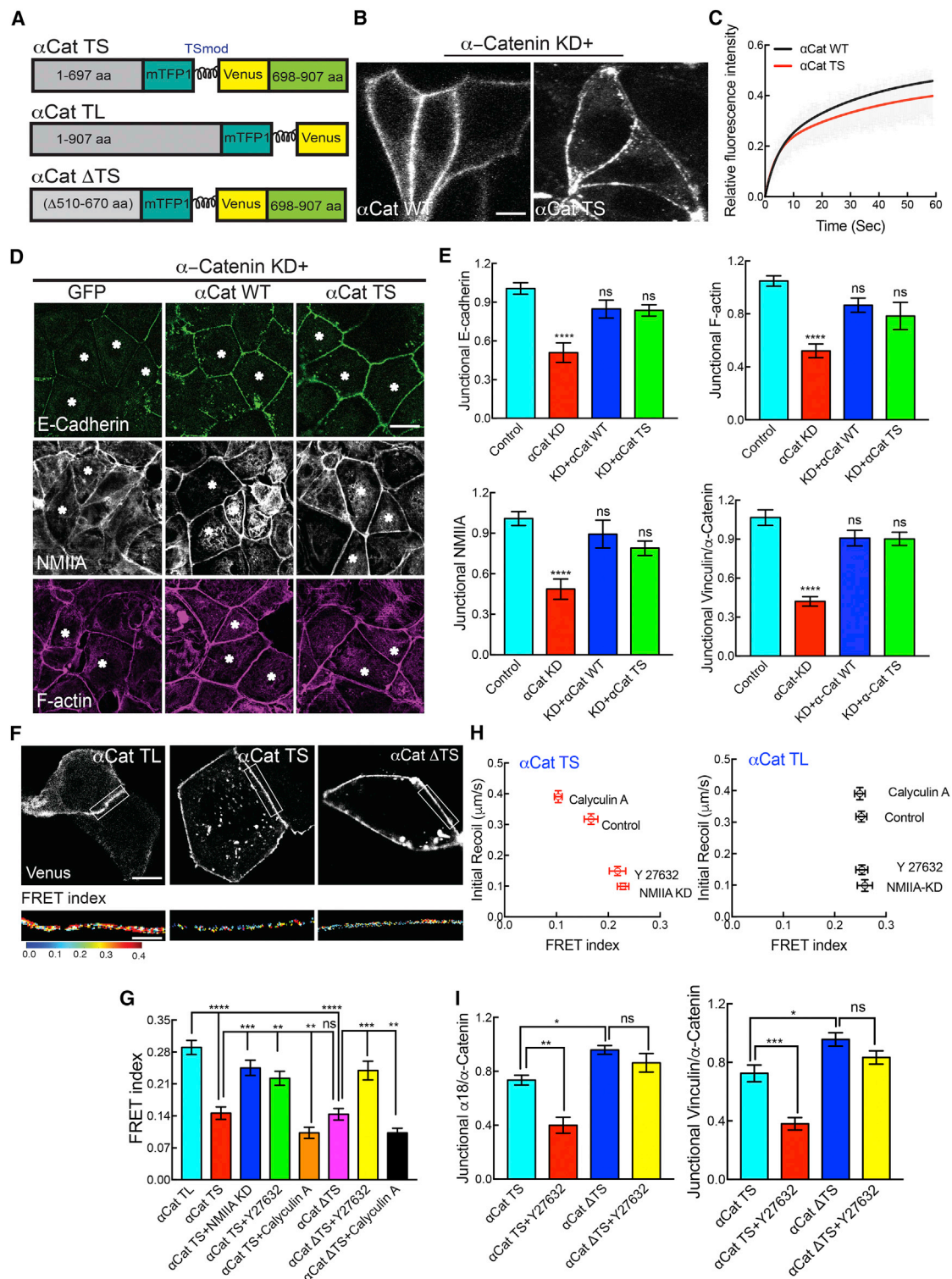
Figure 2. Construction and Validation of an αE-Catenin Tension Sensor

(A) Schematic of the αE-catenin tension sensor constructs (see Results for details).

(B) Apical junctional localization of αE-catenin-GFP (αCat-WT) and αE-catenin tension sensor (αCat TS) expressed in αE-catenin siRNA cells (see also Figure S2A).

(C) FRAP of junctional αCat-WT and αCat-TS expressed in αE-Catenin.

(legend continued on next page)

FMNL2 were principally nuclear (Figure S1B). To assess whether their junctional localization might show interdependence (Peng et al., 2003), we depleted either mDia1 or mDia2 with RNAi (Figures S1C and S1D) and tested whether localization of the other protein was altered (Figure S1E). Small interfering RNA (siRNA) selectively reduced either total mDia1 (Figure S1C) or mDia2 (Figure S1D) by ∼95% and substantially reduced their junctional immunostaining (Figure S1E). Whereas mDia2 was reduced at junctions in mDia1 KD cells, junctional mDia1 was unaffected by mDia2 KD (Figure S1E), implying that mDia1 exerts a dominant influence on the junctional localization of mDia2.

We then used structured illumination microscopy (SIM) to better define the localization of mDia1 at apical junctions (Figure 1D). Polarized Caco-2 cells display actomyosin bundles that lie adjacent to E-cadherin in the apical ZA (Kovacs et al., 2011). mDia1 decorated the junctional membrane between the F-actin bundles (Figure 1D), and this staining pattern was substantially reduced by E-cadherin RNAi (Figure 1E). This suggested that mDia1 was recruited in response to E-cadherin. The ZA is also a prominent site for GTP-RhoA (Priya et al., 2015; Ratheesh et al., 2012), a known activator of mDia1 (Li and Higgs, 2003). Indeed, junctional mDia1 was reduced when RhoA was inactivated with C3-transferase or RNAi (Figure 1E). mDia1 localization was also compromised when we blocked a recently reported feedback network that allows NMII to stabilize the junctional GTP-RhoA zone (Priya et al., 2015), either by NMIIA RNAi or by blocking ROCK with Y-27632 (Figure 1E), keys to the feedback network. Overall, these findings suggest that E-cadherin adhesions may define cortical sites for mDia to accumulate through their ability to establish a stable zone of RhoA signaling at the ZA (Priya et al., 2013). Junctional mDia1 was also blocked by latrunculin A, suggesting that a pre-existing F-actin scaffold might be needed for its recruitment (Figure 1E). As a junctional formin that responded to AJ and RhoA signaling, mDia1 then constituted an interesting candidate to potentially contribute to junctional contractility.

Development of an αE-catenin Tension Sensor

In order to measure molecular-level forces at the interface between E-cadherin adhesions and the actomyosin cytoskeleton, we employed FRET-based TS technology (Grashoff et al., 2010) to develop a probe for tension across αE-catenin (Shapiro and Weis, 2009). We generated a putative force-sensor (αE-Cat-TS) by inserting the TS module between the N-terminal β-catenin binding domain of αE-catenin and its F-actin binding domain (Figure 2A). We postulated that here the TS module would be sensitive to forces exerted from the actomyosin cytoskeleton onto cadherin-bound αE-catenin (Figure S2A). As a negative

control, we inserted the TS module at the very C terminus of αE-catenin (αE-Cat-TL, "tension-less") where, being downstream of the actin-binding domain, it should not experience contractile force (Figures 2A and S2A).

We then expressed αE-Cat-TS in αE-catenin siRNA cells where endogenous protein was reduced by >90% (Figure S2B) and compared its function with that of a GFP-tagged αE-catenin transgene (αE-Cat-WT) expressed at similar levels (Figure S2B). Both constructs localized to cell-cell junctions (Figure 2B) and co-immunoprecipitated E-cadherin (Figure S2C). Further, αE-Cat-TS showed comparable steady-state dynamics to αE-Cat-WT when measured by fluorescence recovery after photobleaching (FRAP) (Figure 2C; Table S2). Importantly, whereas αE-catenin RNAi decreased the amounts of E-cadherin, actomyosin, and vinculin found at apical junctions, these were all restored by αE-Cat-TS as effectively as by αE-Cat-WT (Figures 2D, 2E, and S2D). Overall, these findings established the αE-Cat-TS fusion protein as a functional αE-catenin.

We then tested whether αE-Cat-TS was sensitive to contractile forces. First, we compared FRET across junctional αE-Cat-TS with that across the negative control, αE-Cat-TL (Figures 2F and 2G), which also localized effectively to the ZA. We used a FRET index (described in detail in Experimental Procedures) to correct for variation in transgene expression. αE-Cat-TS displayed a lower FRET index than did αE-Cat-TL, implying that the FRET acceptor/donor pair was further separated in αE-Cat-TS and consistent with the notion that it might be subject to tensile force (Figure 2G). This was supported by the observation that energy exchange across αE-Cat-TS was increased by Y-27632 or NMIIA siRNA (Figures 2G, S2E, and S2F), maneuvers that decrease junctional contractility (Leerberg et al., 2014; Ratheesh et al., 2012). Conversely, Calyculin A, which can stimulate NMII (Cai et al., 2010) and increased junctional recoil in Caco-2 cells (Figures 2H, S2H, and S2I), decreased αCat-TS FRET (Figures 2G and S2F), consistent with an increase in force upon αE-Cat-TS. None of these manipulations affected FRET from αE-Cat-TL (Figure S2G).

To correlate these responses with an independent measure of junctional tension, we performed laser ablation experiments in cells expressing either αE-Cat-TS or αE-Cat-TL (Figures S2H–S2K) and plotted these results against the FRET index data (Figure 2H). These showed a close negative relationship between initial recoil and FRET index for αE-Cat-TS, but not for αE-Cat-TL (Figure 2H), further supporting the notion that αE-Cat-TS was reporting changes in contractile force.

Formally, however, force-induced changes in the proximity of the fluorophores of the TS module could reflect conformational changes in the overall molecule that condition their proximity

(D and E) Representative images (D) and quantitation (E) of E-cadherin, F-actin, NMIIA, and junctional Vinculin/αE-catenin in αE-catenin siRNA cells reconstituted with GFP (left), αE-Cat-WT (center), or αE-Cat-TS (right).

(F) Representative FRET index images of αE-catenin TS constructs.

(G) Effect of manipulating contractility on FRET index for αCat-TS and αE-catenin mutant tension sensor (αCatΔ-TS).

(H) Comparison of FRET index results and junctional recoil when contractility was altered in αE-catenin siRNA cells reconstituted with either αCat-TS or αCat-TL.

(I) Contractile sensitivity of α18 mAb (left) and vinculin (right) staining (normalized to αE-catenin) at the ZA in αE-catenin siRNA cells reconstituted with either αCat-TS or αCatΔ-TS.

Data are means ± SEM (n = 3 independent experiments). For FRAP analysis, 20–25 junctions were analyzed per condition per experiment. ns, not significant, *p < 0.05, **p < 0.01,***p < 0.001, and ****p < 0.0001; one-way ANOVA with Dunnett's post hoc test (E and G) and Sidak's post hoc test (I). Scale bars represent 10 μm (B, D, and F) and 2 μm (F, cropped region). See also Figure S2 and Tables S1 and S2.

rather than tensile stretching of the protein linker that separates them. This alternative possibility is pertinent in the case of αE-catenin, which increasingly appears to be able to exist in an auto-inhibited conformation (Choi et al., 2012), where vinculin binding and the epitope recognized by the α-18 mAb are masked, as well as in an "open" configuration that can be promoted by contractile force (Yonemura et al., 2010). Consistent with this notion, vinculin recruitment to the ZA is force sensitive in Caco-2 cells (Leerberg et al., 2014), as is α-18 mAb staining, which was decreased by Y-27632 or NMIIA KD and increased by Calyculin A (Figures S2M and S2N).

To discriminate between these possibilities, we designed a further deletion construct (αE-CatΔ-TS, Figure 2A) lacking residues 510–670 of αE-catenin, which are reported to be necessary for the vinculin and α-18 mAb binding sites to be masked by the "closed" conformation (Yonemura et al., 2010). This deletion mutant localized effectively to AJs (Figure 2F). We then immunolabeled cells expressing αE-CatΔ-TS with both anti-vinculin and α18 mAbs to test the prediction that this mutant exists in the "open" conformation. αE-catenin KD cells reconstituted with αE-CatΔ-TS displayed higher baseline levels of junctional vinculin and α18 mAb than did cells expressing αE-Cat-TS (Figure 2I). Furthermore, labeling for both markers was decreased by Y-27632 in αE-Cat-TS cells, consistent with these being force dependent, but not in αE-CatΔ-TS cells. Overall, these support the conclusion that the αE-CatΔ-TS mutant exists in an open configuration that is independent of force, as previously proposed (Yonemura et al., 2010).

We then compared the FRET response of αE-CatΔ-TS with that of αE-Cat-TS (Figure 2G). If the FRET changes in the reporters were dominated by conformational changes, rather than stretch of the reporter, we predicted that energy exchange across αE-CatΔ-TS would be lower at baseline than that of the constitutively "open" αE-CatΔ-TS. Further, when contractility was inhibited, FRET would increase across αE-Cat-TS but not across αE-CatΔ-TS. Instead, we found that both reporters showed similar degrees of energy transfer at baseline, which also increased comparably when contractility was inhibited with Y-27632. Finally, Calyculin A decreased energy exchange across αE-CatΔ-TS as it did for αE-Cat-TS (Figures 2G and S2L). The indistinguishable behaviors of the wild-type (WT) and constitutively "open" reporters implied that in both contexts the TS module was principally responding to changes in tension rather than changes in conformation.

mDia1 Supports Junctional Tension at the ZA
We then applied these assays to mDia1 KD cells (Figure 3). Using laser ablation, we found that instantaneous recoil of E-cadherin-tagRFP-T at vertices was substantially reduced in mDia1 KD cells (Figures 3A and 3B), without significant change in k-values (Table S1). Recoil was restored by expression of exogenous RNAi-resistant GFP-mDia1 (Figures 3A, 3B, and S1C), confirming a specific effect. In contrast, FMNL2 siRNA did not alter junctional recoil (Figures S3A–S3C).

We then used αE-Cat-TS reconstituted into αE-catenin KD cells to test whether mDia1 affected molecular-level forces at the cadherin adhesion complex. Energy transfer was increased significantly across αE-Cat-TS when mDia1 was depleted by

siRNA (Figure 3D), correlating negatively with the change in initial recoil (Figure 3E), and this was corrected by expression of mCherry-mDia1 (Figures 3C–3E). Furthermore, the constitutively "open" αE-CatΔ-TS responded identically (Figures S3D and S3E), reinforcing the conclusion that mDia1 KD was altering tension across αE-catenin. In support, α18 mAb (Figures 3F and 3G) and vinculin (Figures 3F and 3H) at the ZA were also reduced upon mDia1 depletion and restored by expression of GFP-mDia1. Overall, these findings implicate mDia1 in generating contractile force at the ZA. They further imply that, while other formins may localize to junctions, they did not compensate to support contractility when mDia1 was depleted.

mDia1 KD Disturbs the Stability and Organization of Junctional NMII
To begin to understand how mDia1 supported junctional contractility, we first examined junctional NMII. Junctional NMIIA (Figures 4A and 4B) and, to a lesser extent, NMIIB (Figures 4A and 4C) were reduced in mDia1 KD cells. Further, GFP-NMIIA turnover was increased in mDia1 KD cells, as reflected in an increased mobile fraction by FRAP (Figure 4D; Table S2). This suggested that mDia1 might stabilize NMII at the junctions.

Then we examined the organization of NMIIA at the ZA by SIM. In control cells, NMIIA localized in puncta that aligned with the perijunctional actin bundles (Figure S3F), whereas NMIIA puncta appeared more dispersed at mDia1 KD junctions. We then expressed GFP-NMIIA in Caco-2 cells and used its native GFP fluorescence to visualize the N termini of the molecules along with indirect immunofluorescence to identify antibodies directed against the C termini of NMIIA (Beach et al., 2014; Ebrahim et al., 2013). As shown previously (Michael et al., 2016), this revealed alternating patterns (green-red-green) consistent with the head-tail-head disposition of NMII minifilaments (Figures 4F and S4A). We then quantitated the orientation of NMIIA minifilaments by measuring the angle between the axis of a minifilament and the junction (Figure S4B). In control cells, the majority of NMIIA minifilaments aligned parallel to junctions (Figure 4G) with a limited dispersion (SD) of minifilament angles (Figure 4H). In contrast, in mDia1 KD cells, myosin minifilaments were located further away from the junctions (Figure 4I) and displayed a much greater dispersion of angles (Figures 4G and 4H). Minifilament length, however, was unaltered (Figure 4J). Overall, these observations suggest that mDia1 KD did not affect the ability of cells to form NMIIA minifilaments but profoundly disturbed their distribution and stability at the junctions.

mDia1 Is Necessary for Dynamic Stability of the Junctional Actin Cytoskeleton
As F-actin conditions the recruitment of NMII to the ZA (Verma et al., 2012), we then asked how the junctional actin cytoskeleton was affected in mDia1 KD cells. The junctional cortex is distinguished by populations of dynamic actin filaments, which are nucleated at the junctional membrane and then become reorganized and incorporated into the prominent perijunctional bundles that run adjacent to the ZA (Michael et al., 2016; Kovacs et al., 2011).

We found that mDia1 KD profoundly disturbed the junctional cytoskeleton at the ZA (Figure 5A). Steady-state F-actin levels
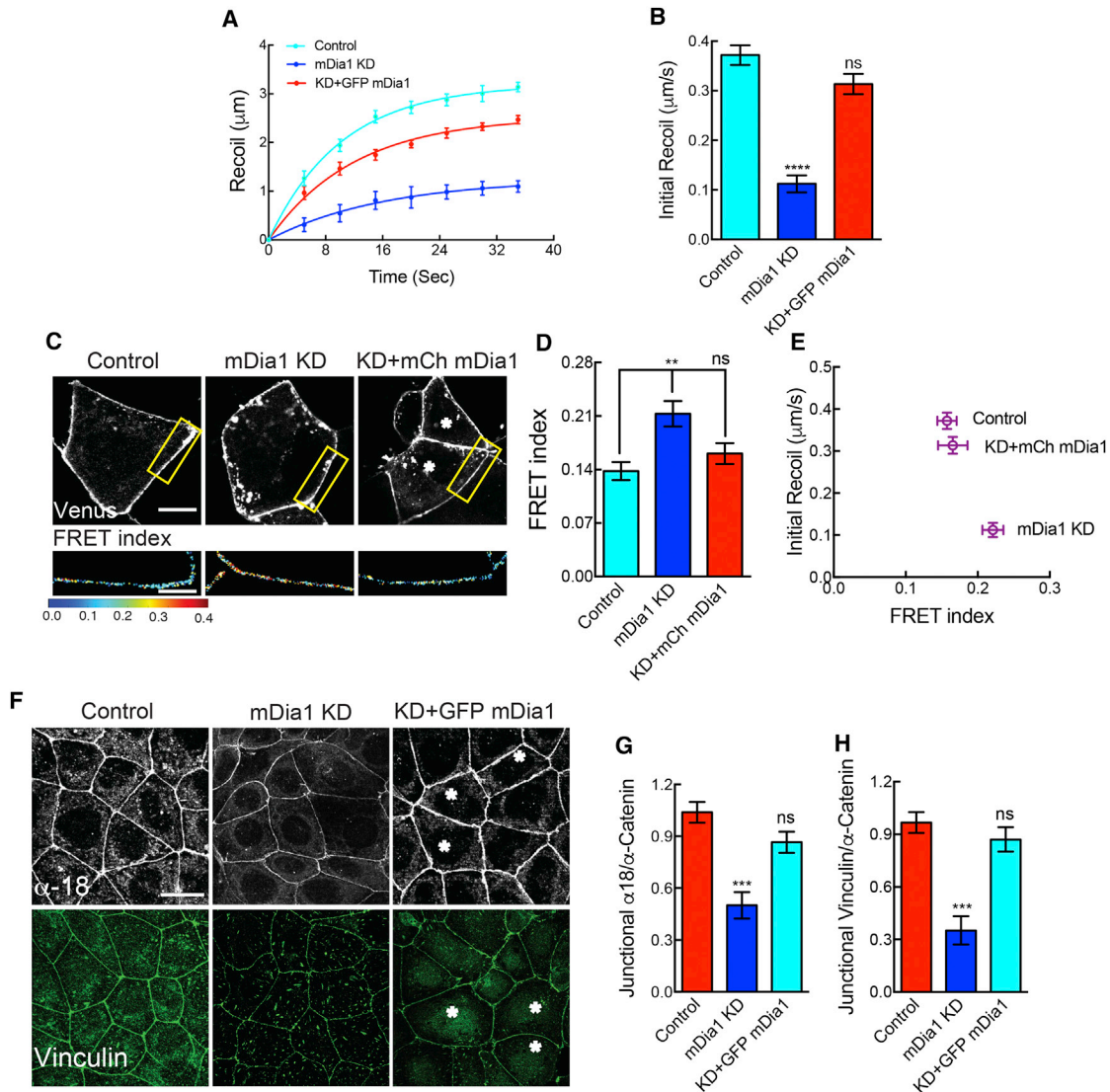
Figure 3. mDia1 Supports Contractile Tension at the Zonula Adherens

(A and B) Effect of mDia1 KD or reconstitution with RNAi-resistant GFP-mDia1 on vertex recoil (A) and initial recoil velocities (B) at the ZA after laser ablation of E-cadherin-TagRFP-T junctions (25–30 junctions/condition/n; n = 3).

(C and D) Effect of mDia1 KD and its reconstitution on FRET index across αCat-TS at the ZA. Representative images (C) and quantitation (D) are shown.

(E) Effect of mDia1 KD (and reconstitution) on αCat-TS FRET index compared to laser ablation (initial recoil velocity) assays.

(F–H) Representative images (F) and fluorescence quantitation (normalized to αE-catenin) for α18 mAb (G) and vinculin (H) staining at the ZA in mDia1 KD and reconstituted cells.

Data are means ± SEM from n = 3 independent experiments. ns, not significant, *p < 0.05, ***p < 0.001, ****p < 0.0001, one-way ANOVA with Dunnett's post hoc test. Scale bars represent 10 μm (C and F) and 2 μm (cropped region on C). See also Figure S3 and Table S1.

were reduced (Figures 5A and 5B), and, more strikingly, SIM imaging revealed qualitative changes in actin network organization (Figure 5A). The prominent F-actin bundles found at the ZA in control cells were replaced with a more dispersed network that appeared to extend from the membrane into the cytoplasm. To quantitate this change in organization, we used a recently described approach to skeletonize F-actin patterns and measured the number of overlapping intersects that were found in image fields of defined size (Michael et al., 2016). Indeed, the

density of intersects was significantly increased by mDia1 KD and restored by expression of RNAi-resistant GFP-mDia1 (Figure 5C).

mDia1 KD also affected the dynamics of the junctional cytoskeleton. Levels of fluorescent G-actin incorporation at junctions were reduced in mDia1 KD cells (Figure 5D), suggesting that mDia1 might contribute to nucleation or protect barbed ends from capping at these sites (Goode and Eck, 2007). In FRAP studies, mDia1 KD significantly increased the mobile fraction
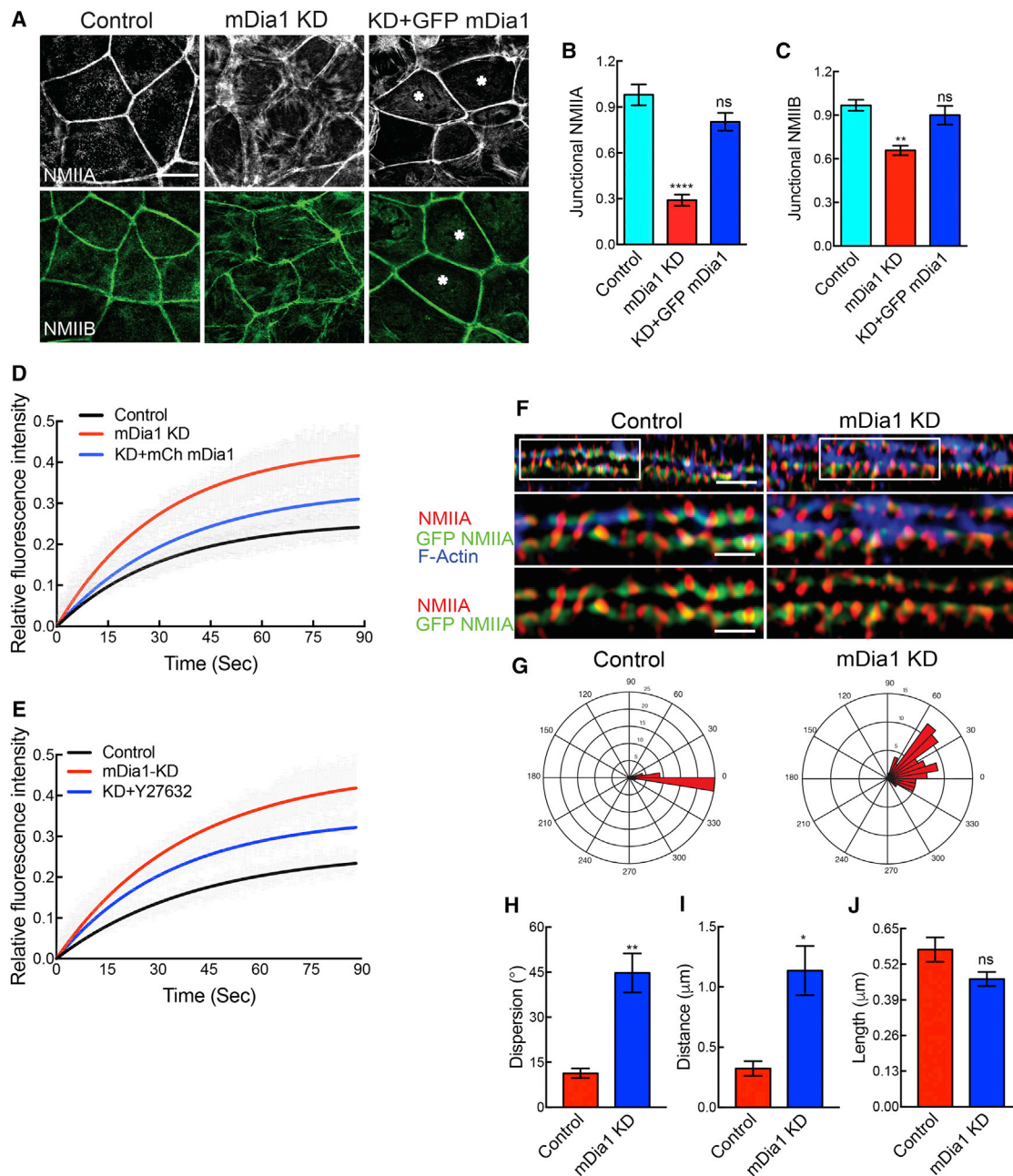
Figure 4. mDia1 Regulates Myosin II Organization and Stability at the ZA

(A–C) Impact of mDia1 KD or reconstitution on junctional NMII. Representative confocal images (A) and quantitation for NMIIA (B) and NMIIB (C) are shown.

(D) FRAP of transiently expressed GFP-NMIIA.

(E) Effect of Y-27632 on FRAP of GFP-NMIIA in mDia1 KD cells.

(F–J) Effect of mDia1 KD on junctional NMIIA minifilament organization. Representative SIM images (F), polar histogram plots of minifilament orientation respect to the junction (G), dispersion (H), distance from junction (I), and minifilament length (J) are shown.

Data are means ± SEM from n = 3 independent experiments. For FRAP, 20–25 junctions were analyzed/condition/experiment. ns, not significant, *p < 0.05, **p < 0.01, ***p < 0.001, and ****p < 0.0001; unpaired t-Test with Welch's correction (H–J) or one-way ANOVA with Dunnett's post hoc test (B and C). Scale bars represent 10 μm (A), 5 μm (F), and 2 μm (F, cropped region). See also Figure S4 and Table S2.

of GFP-actin at the ZA, accompanied by a decrease in the half-life ($T_{1/2}$) of recovery (Figure 5E; Table S2), suggesting that junctional F-actin had become significantly more dynamic. To pursue this, we then measured fluorescence decay after activation of actin tagged with photoactivatable GFP (PAGFP-actin). Fluorescence decay was accelerated in the mDia1 KD cells compared
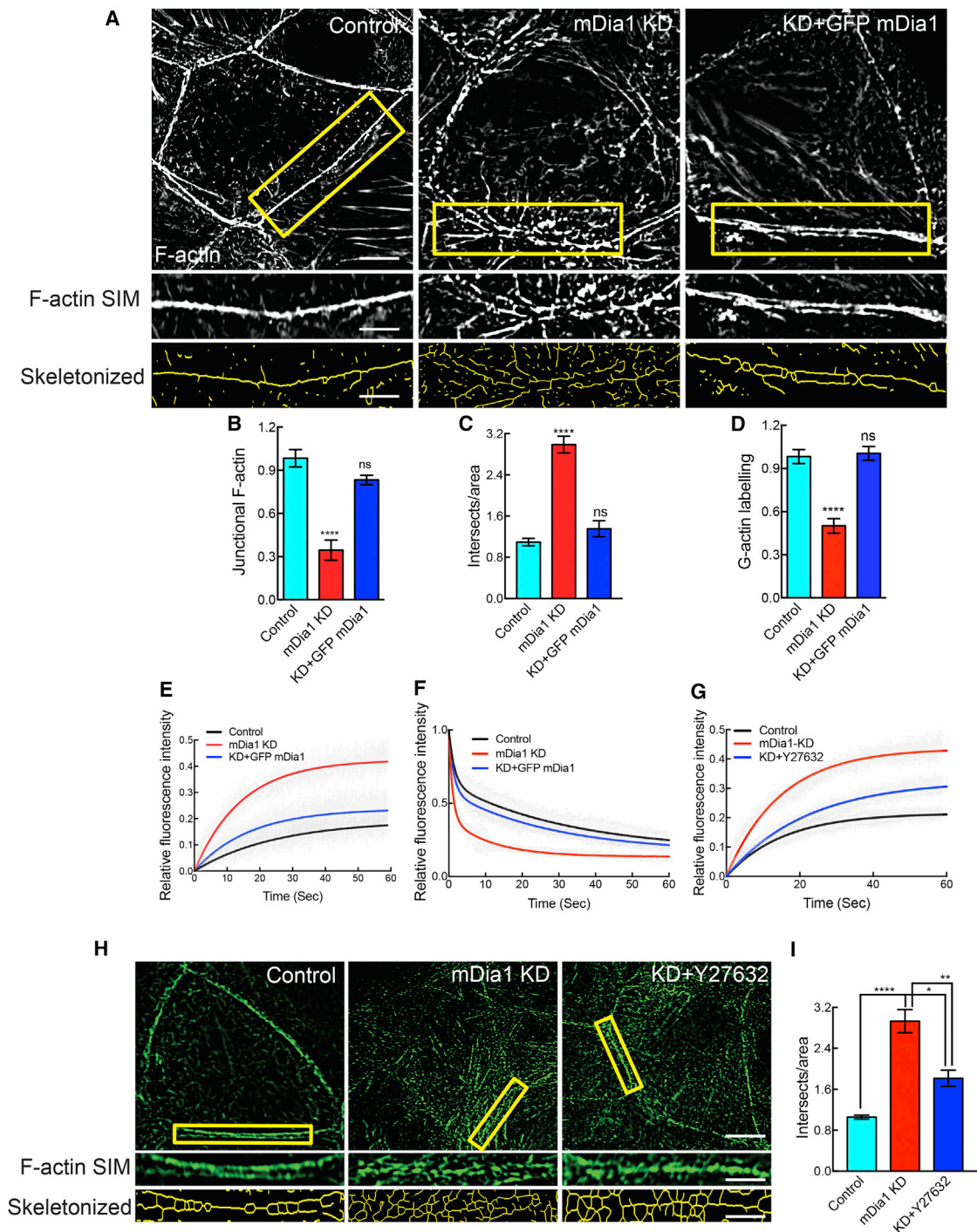
Figure 5. mDia1 Supports Architectural Organization and Stability of F-actin at the ZA

(A–C) Effect of mDia1 KD or its reconstitution on F-actin at the ZA. (A) Representative SIM images with magnified views of the boxed areas are shown with the corresponding skeletonization analysis. Quantitation of F-actin intensity (B) and organization (C) based on skeletonization analysis is shown.

(D) Free barbed ends at the ZA labeled with Alexa 594-G-actin.

(E) Effect of mDia1 KD on FRAP of transiently expressed GFP-Actin.

(F) Junctional actin filament stability measured by fluorescence decay after photoactivation of mRFP-PA-GFP-actin.

(G) Y-27632 ameliorates the effect of mDia1 KD on turnover of GFP-actin measured by FRAP.

(H) Representative images of F-actin architecture in control, mDia1 KD, and mDia1 KD cells treated with Y27632, with magnified views of the boxed areas and corresponding skeletonized images.

(legend continued on next page)

with controls (Figure 5F; Table S3), reinforcing the concept that mDia1 promotes actin filament stability at the ZA. Overall, this suggested that mDia1 played a necessary role in supporting dynamic stability and organization of the junctional actin cytoskeleton.

Junctional Actomyosin Is More Sensitive to Stress-Induced Destabilization in mDia1 KD Cells

Together, these observations implied that in mDia1 KD cells NMIIA minifilaments associate with F-actin networks that are more disorganized than those found in control cells. Disorganization can predispose F-actin networks to stress-induced fragmentation and severing (Murrell et al., 2015; Reymann et al., 2012; Haviv et al., 2008). We therefore wondered whether the destabilization of junctional actomyosin that we found in mDia1 KD cells might reflect the impact of NMII acting on a more disorganized F-actin network. Indeed, we found that the enhanced turnovers of both GFP-actin (Figure 5G) and GFP-NMIIA (Figure 4E) seen in mDia1 KD cells were ameliorated by Y-27632. Furthermore, Y-27632 caused the polydispersed junctional F-actin networks of mDia1 KD cells to become more compact and better organized (Figures 5H and 5I). Together, these observations suggested that architectural reorganization by mDia1 helps the junctional F-actin network resist stress-induced turnover and thereby stabilizes actomyosin.

mDia1 Promotes Network Reorganization during Biogenesis of the Junctional Cortex

To pursue this possibility, we then analyzed how the junctional actin cytoskeleton of mDia1 KD cells reassembled after it had been disrupted by latrunculin A. We recently found that network reorganization is a prominent feature of this process, where initially polydisperse F-actin networks are converted into co-linear bundles (Michael et al., 2016).

To test this, we used skeletonization analysis to quantitate F-actin network organization. As previously observed (Michael et al., 2016; Tang and Brieher, 2012), junctional F-actin networks recover from residual, latrunculin-resistant puncta that are found at cell-cell junctions (Figures 6A and S4C). The initial phase (0–30 min) is insensitive to SMIFH2 (Michael et al., 2016) and yields a dispersed network with a relatively large number of F-actin intersects that progressively decrease in number over 60–90 min, as the co-linear bundles form (Figures 6A and 6C). In contrast, mDia1 KD cells displayed a higher number of intersects at 30 min, and this did not decrease with time (Figures 6A and 6C). This was accompanied by defects in NMIIA minifilament organization (Figure 6B). Control cells initially recruited NMIIA minifilaments that were relatively dispersed (Figures 6B and 6D). But as actin reorganization occurred, the dispersion of NMIIA minifilaments decreased, and these came progressively closer to the junctional membrane (Figures 6B, 6D, and 6E). In mDia1 KD cells, however, although their length was not altered (Figure 6F), NMIIA minifilaments retained a dispersed distribution (Figure 6D), located further away from the junction (Figure 6E), throughout the assay. Overall, these findings support the concept that mDia1 contributes to the architectural reorganization of both F-actin and NMII that is needed to build an effective contractile apparatus.

Functional Impact of mDia1 in Established Epithelial Monolayers

As its junctional recruitment depended on E-cadherin, manipulating mDia1 provided an opportunity for us to test how the generation of contractility at the ZA might affect epithelial integrity in established Caco-2 monolayers (Figures 7 and S5). Although AJs formed between mDia1 KD cells (Figure S5A), the amount of E-cadherin that concentrated to form an apical ZA was significantly reduced (Figure S5A), without change in the total or surface levels of E-cadherin (Figure S5B). Together, these findings suggested that mDia1 promotes the concentrated localization of E-cadherin to form the ZA, consistent with earlier evidence that implicated contractility in stabilizing E-cadherin to form the ZA (Wu et al., 2014; Priya et al., 2013; Ratheesh et al., 2012; Smutny et al., 2010; Homem and Peifer, 2008).

Further, we found that although TJs formed in mDia1 KD cells, the junctional levels of their constituent proteins, ZO-1, occludin, and Par3, were all significantly reduced compared with controls (Figures 7A and 7B). As contractility stabilizes E-cadherin at the ZA (Priya et al., 2013), we wondered whether the ability of mDia1 to support junctional contractility might also affect the stability of TJ components. Indeed, FRAP revealed that the mobile fractions of both ZO-1-Emerald (Figures 7C and 7D) and occludin-Emerald (Figures 7E and 7F) were increased in mDia1 KD cells. The notion that contractility might stabilize these TJ components was further supported by finding that Y-27632 alone decreased the steady-state junctional levels of ZO-1 and occludin (Figures 7B and S5C) and also increased their mobile fractions (Figures 7C–7E).

As the TJ constitutes a key barrier to the transepithelial flux of solutes and macromolecules (Marchiando et al., 2010), we then tested how mDia1 KD affected epithelial permeability. Measured by transepithelial resistance (TER) to ionic flux, barrier integrity increased progressively during culture to reach a plateau at ~16 days (Figure 7G). In contrast, TER remained significantly lower in mDia1 KD cells (Figures 7G and 7H). Furthermore, transepithelial flux of 4 kDa dextran was significantly higher in mDia1 KD cells than in controls (Figure 7I). Therefore, although mDia1 KD cells were able to assemble TJs, their ability to seal the paracellular pathway was compromised. Furthermore, the epithelial barrier of Caco-2 monolayers was also significantly reduced when contractility was inhibited with Y-27632 alone (Figures 7G–7I).

Collectively, these data suggested that basal TJ function in established monolayers might be conditioned by the ability of

---

(I) Skeletonization analysis of F-actin organization.
Data are means ± SEM (n = 3 independent experiments). For FRAP and photoactivation, 20–25 junctions were analyzed/condition/experiment. ns, not significant, *p < 0.05, **p < 0.01, ****p < 0.0001; one-way ANOVA with Dunnett's post hoc test (B–D) and Sidak's post hoc test (I). Scale bars represent 5 μm (A and H) and 2 μm (cropped, H). See also Tables S2 and S3.
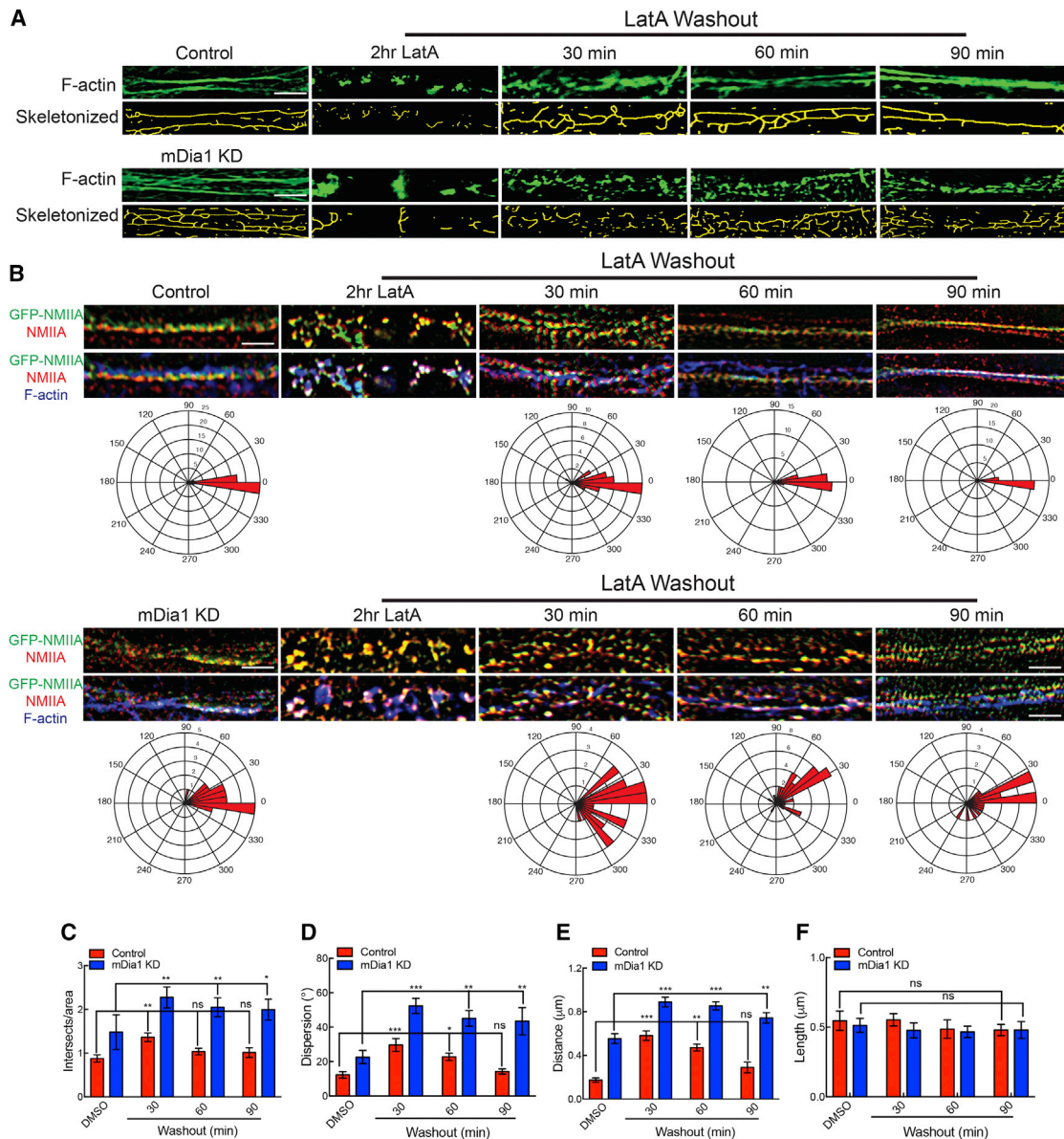
Figure 6. mDia1 Mediates Network Architectural Reorganization during Cytoskeletal Biogenesis at the ZA

Effect of mDia1 KD on F-actin and NMIIA minifilament organization as the junctional actomyosin cytoskeleton reassembles following Latrunculin A wash out is shown.

(A) Representative SIM and skeletonization images (cropped regions from images shown in Figure S4C).

(B) Representative SIM and polar histogram plots of NMIIA minifilament distribution relative to the junctional membrane.

(C) Skeletonization analysis of F-actin organization.

(D–F) NMIIA minifilament dispersion (D), distance (E), and length (F).

Data are means ± SEM from n = 3 independent experiments. ns, not significant, *p < 0.05, **p < 0.01 and ***p < 0.001; one-way ANOVA with Dunnett's post hoc test (C–F). Scale bars represent 2 μm (A and B). See also Figure S4.

mDia1 to support junctional contractility at the TJs, as well as at the ZA. Consistent with this, mDia1 co-accumulated with ZO-1 at TJs (Figure S5D), proximate to the actomyosin (Figure S5E) that is found in this region (Fanning et al., 2012). Moreover, actomyosin at the TJs was disrupted in mDia1 KD cells (Figure S5E). However, the level of mDia1 observed with ZO-1 at the TJs was reduced by E-cadherin KD (Figure S5F),

suggesting that it might reflect initial cadherin-dependent recruitment to the ZA.

Finally, since increased sensitivity to contractile stress contributed to destabilizing junctional actomyosin in mDia1 KD cells (Figures 4E and 5G–5I), we wondered whether a similar sensitization to NMII also affected the TJs. To test this, we asked whether Y-27632 could ameliorate the TJ defects in mDia1 KD
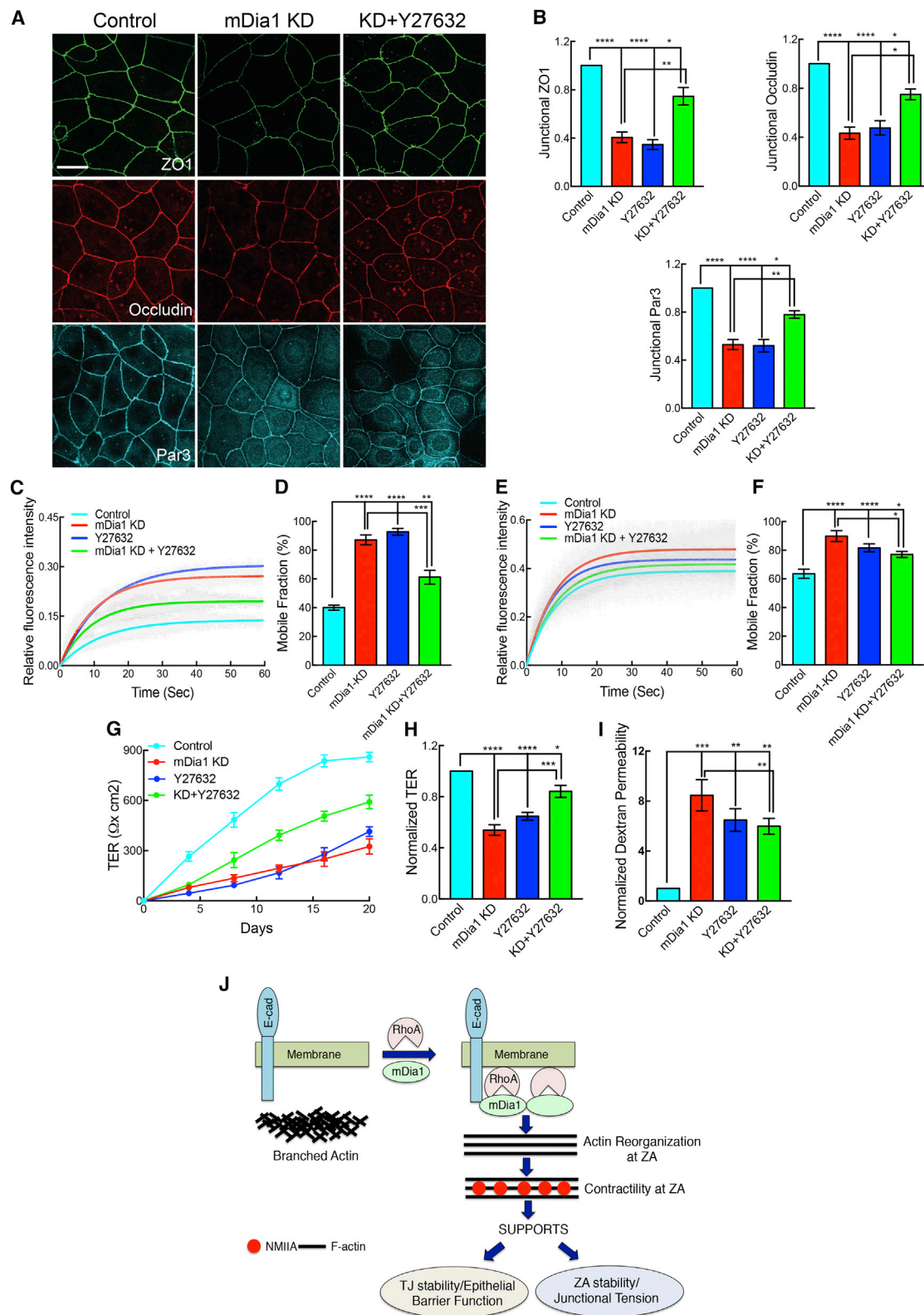
Figure 7. mDia1 Supports Tight Junction Stability and Barrier Integrity

Effects of mDia1 KD, Y-27632 alone, or in combination on TJs.

(A and B) Representative confocal images (A) and quantitation (B) of ZO-1, occludin, and Par3.

(legend continued on next page)

cells, as it did for actomyosin at the ZA (Figures 4E and 5G–5I). Indeed, we found that Y-27632 partially rescued the junctional level of TJ proteins (Figure 7B) and also stabilized ZO-1-Emerald and occludin-Emerald in mDia1 KD cells (Figures 7C–7F). Further, Y-27632 restored the TER in mDia1 KD cells to levels approaching those of controls and higher than seen with either mDia1 KD or Y-27632 alone (Figures 7G and 7H). Y-27632 also partially restored dextran permeability in mDia1 KD cells (Figure 7I). Together, these results suggest that the contribution of mDia1 to epithelial barrier function reflects its ability to generate actin networks that are optimized to resist stress and can thereby effectively generate contractility to stabilize TJs as well as AJs.

DISCUSSION

Our present study yields three major conclusions. First, mDia1 is recruited to the junctional cortex in response to E-cadherin adhesion and RhoA, where it plays a major role in generating junctional contractility. For these experiments, we complemented a suite of assays for junctional tension with an αE-catenin tension sensor. Although it was possible that conformational change in the αE-catenin backbone might influence energy exchange across the sensor, this seems unlikely, as αE-Cat-TS behaved identically to a mutant αE-Cat-TS reporter that was designed to be constitutively open. Together, our results support evidence that Diaphanous regulates junctional myosin in the fly embryo (Homem and Peifer, 2008) and reinforce the concept that mechanical force is an important regulator of αE-catenin (Buckley et al., 2014; Yao et al., 2014; Yonemura et al., 2010) that can affect processes such as junctional actin dynamics (Leerberg et al., 2014).

Second, mDia1 facilitates the cellular process of network architectural reorganization that allows the dynamic cytoskeleton to generate actomyosin bundles at the ZA (Michael et al., 2016). Thus, mDia1-deficient cells failed to assemble perijunctional bundles, displaying instead a disorganized pattern akin to that seen before nascent networks undergo architectural reorganization (Michael et al., 2016). Indeed, in latrunculin wash-out experiments, junctional F-actin reassembled but failed to reorganize into bundles when mDia1 was depleted. A key effect of this architectural regulation is to enhance the resistance of F-networks to the stress of NMII binding. Disorganized actin networks are both inefficient scaffolds for force generation and also more sensitive to stress-induced severing (Murrell et al., 2015; Reymann et al., 2012; Haviv et al., 2008). Consistent with this, we found that the distribution of NMIIA minifilaments was also disorganized at the junctional cortex of mDia1 KD cells. Further, the destabilization of both junctional F-actin and NMIIA seen in mDia1 KD cells was largely corrected when contractility was blocked with Y-27632.

Altogether, these suggest that many abnormal features of the mDia1-deficient junctional cytoskeleton reflect how mDia1 regulates actin network architecture to allow it to withstand contractile stress. Whether mDia1 nucleates non-branched filaments de novo (Bovellan et al., 2014) or works on filaments that are initiated by another nucleator (Breitsprecher et al., 2012), such as Arp2/3, remains to be elucidated. We favor the second hypothesis, as Arp2/3 inhibition compromises the formation of contractile bundles (Verma et al., 2012), and SMIFH2 did not affect the initial phase of actin reassembly in latrunculin wash-out experiments (Michael et al., 2016; Tang and Brieher, 2012). If so, then mDia1 might cooperate with a mechanism to debranch Arp2/3-nucleated networks, such as might be provided by Coronin 1B (Cai et al., 2008), which also participates in architectural reorganization (Michael et al., 2016).

Third, mDia1 stabilized proteins of both the AJs and TJs to control epithelial permeability. This impact on E-cadherin is consistent with earlier evidence that RhoA-dependent contractility stabilizes E-cadherin (Smutny et al., 2010; Priya et al., 2013). As junctional requires cadherin adhesion to couple the contractile cortices of cells together (Priya and Yap, 2015), stabilization of E-cadherin may also have contributed to the ability of mDia1 to support tension at the ZA. However, the functional impact of mDia1-dependent contractility was not confined to the ZA. Although mDia1 KD cells formed TJs, their protein content was reduced, and their epithelial barrier to ions and small macromolecules was compromised. Whereas earlier studies reported that epithelial permeability was increased when cellular contractility is stimulated (Marchiando et al., 2010; Blair et al., 2006; Turner et al., 1997), our present results reinforce the complementary notion that junctional contractility also supports steady-state TJs (Kannan and Tang, 2015; Nusrat et al., 1995). Physical connections between TJ plaques and perijunctional bundles (Madara, 1987) might allow tension to be transmitted to stabilize dynamic TJ components (Shen et al., 2008), akin to what is seen for E-cadherin at the ZA (Priya et al., 2013). Indeed, we found that the turnover of both ZO-1 and occludin was increased by mDia1 KD and also by Y-27632. How molecular stability of TJ components may be influenced by contractile force will be an interesting issue for future research.

We therefore propose that E-cadherin-dependent RhoA signaling recruits mDia1 to establish effective contractility at the ZA, which ramifies to affect other components of the apical junction complex (Figure 7J). Together, these findings provide new insights into how AJ contractility contributes to epithelial biology. First, they imply that the junctional contractility evident even for morphogenetically stable monolayers supports their function as tissue barriers. Second, our findings provide insight on the functional interrelationship between cadherin adhesion and TJs. Earlier studies reported that cadherin adhesion may support TJ biogenesis in some (Tunggal et al., 2005; Wheelock

(C–F) FRAP of ZO-1-Emerald (C and D) and Occludin-Emerald (E and F). Recovery curves (C and E) and mobile fractions (D and F) are shown.
(G–I) Effect on development of transepithelial electrical resistance (TER) (G), normalized TER (H), and transepithelial dextran flux (I) after 20-day culture.
(J) Model of mDia1 as a necessary facilitator of E-cadherin-based contractility that stabilizes AJs and TJs to promote cell-cell adhesion and the integrity of epithelial barriers, respectively. See also Figure S5 and Table S2.
Data are means ± SEM from n = 3 independent experiments. ns, not significant, For FRAP analysis, 20-25 junctions were analyzed per condition per experiment; *p < 0.05, **p < 0.01, ***p < 0.001, and ****p < 0.0001; one-way ANOVA with Sidak's post hoc test (B, D, F, H, and I). Scale bars represent 10 μm (A and B).

and Jensen, 1992; Gumbiner et al., 1988), but not all (Capaldo and Macara, 2007; Ohsugi et al., 1997), circumstances. We suggest that the impact of E-cadherin on TJs may reflect not just adhesion but also an impact of the contractile cytoskeleton that cadherin adhesion establishes. Finally, previous efforts to understand how contractility can regulate epithelial barrier function have focused on elucidating the role of myosin regulation (Marchiando et al., 2010). Our data highlight the importance of mechanisms, such as mDia1, that allow actin networks to resist stress for effective contractility. More broadly, our findings, taken with their role in the biogenesis of junctional actomyosin (Michael et al., 2016; Jodoin et al., 2015; Homem and Peifer, 2008), suggest that actin regulators can provide complementary targets to control barrier function both in health and disease.

EXPERIMENTAL PROCEDURES

Construction of TS Plasmids

The TS module with mTFP1-F40-venusA206K was adapted from Vinculin TS (a kind gift from Martin Schwartz [Grashoff et al., 2010]). The TSmod was cloned in to pEGFP-N1 vector at Xho1 and Not1 restriction sites. For αE-Cat-TS, the mouse N-terminal (1–697 aa) of αE-catenin was inserted before mTFP1 by infusion cloning (Takara Bioscience, Clontech) at the Xho1 restriction site. The C-terminal fragment (698–906 aa) of αE-catenin was similarly cloned after VenusA206K at the Not1 restriction site. For αE-Cat-TL, the full-length αE-catenin (1–906) was inserted at the Xho1 site, and a stop codon is inserted after VenusA206K in the plasmid. For αE-CatΔ-TS, the αE-Cat-TS was digested with NheI and XmaI to cut out a fragment corresponding to 1–670 aa, and a PCR-amplified fragment corresponding to amino acids 1–509 from mouse αE-catenin was ligated back at the same restriction enzyme sites. All clones were confirmed by sequencing.

SUPPLEMENTAL INFORMATION

Supplemental Information includes Supplemental Experimental Procedures, five figures, four tables, and one movie and can be found with this article online at http://dx.doi.org/10.1016/j.celrep.2017.02.078.

AUTHOR CONTRIBUTIONS

The project was conceived by B.R.A., S.K.W., and A.S.Y.; experiments were performed by B.R.A., S.K.W., and Z.Z.L.; G.A.G. developed FRET, ablation, and actomyosin minifilament analysis tools and the design of the αE-Cat TS together with B.R.A.; R.G.P., S.W.G., and A.D.B. contributed expertise; the paper was written by B.R.A., G.A.G., and A.S.Y. and approved by all the authors.

REFERENCES

Anderson, J.M., and Van Itallie, C.M. (2009). Physiology and function of the tight junction. Cold Spring Harb. Perspect. Biol. *1*, a002584.

Beach, J.R., Shao, L., Remmert, K., Li, D., Betzig, E., and Hammer, J.A., 3rd. (2014). Nonmuscle myosin II isoforms coassemble in living cells. Curr. Biol. *24*, 1160–1166.

Blair, S.A., Kane, S.V., Clayburgh, D.R., and Turner, J.R. (2006). Epithelial myosin light chain kinase expression and activity are upregulated in inflammatory bowel disease. Lab. Invest. *86*, 191–201.

Bovellan, M., Romeo, Y., Biro, M., Boden, A., Chugh, P., Yonis, A., Vaghela, M., Fritzsche, M., Moulding, D., Thorogate, R., et al. (2014). Cellular control of cortical actin nucleation. Curr. Biol. *24*, 1628–1635.

Breitsprecher, D., Jaiswal, R., Bombardier, J.P., Gould, C.J., Gelles, J., and Goode, B.L. (2012). Rocket launcher mechanism of collaborative actin assembly defined by single-molecule imaging. Science *336*, 1164–1168.

Buckley, C.D., Tan, J.L., Anderson, K.L., Hanein, D., Volkmann, N., Weis, W.I., Nelson, W.J., and Dunn, A.R. (2014). Cell adhesion. The minimal cadherin-catenin complex binds to actin filaments under force. Science *346*, http://dx.doi.org/10.1126/science.1254211.

Cai, L., Makhov, A.M., Schafer, D.A., and Bear, J.E. (2008). Coronin 1B antagonizes cortactin and remodels Arp2/3-containing actin branches in lamellipodia. Cell *134*, 828–842.

Cai, Y., Rossier, O., Gauthier, N.C., Biais, N., Fardin, M.A., Zhang, X., Miller, L.W., Ladoux, B., Cornish, V.W., and Sheetz, M.P. (2010). Cytoskeletal coherence requires myosin-IIA contractility. J. Cell Sci. *123*, 413–423.

Capaldo, C.T., and Macara, I.G. (2007). Depletion of E-cadherin disrupts establishment but not maintenance of cell junctions in Madin-Darby canine kidney epithelial cells. Mol. Biol. Cell *18*, 189–200.

Carramusa, L., Ballestrem, C., Zilberman, Y., and Bershadsky, A.D. (2007). Mammalian diaphanous-related formin Dia1 controls the organization of E-cadherin-mediated cell-cell junctions. J. Cell Sci. *120*, 3870–3882.

Choi, H.J., Pokutta, S., Cadwell, G.W., Bobkov, A.A., Bankston, L.A., Liddington, R.C., and Weis, W.I. (2012). αE-catenin is an autoinhibited molecule that coactivates vinculin. Proc. Natl. Acad. Sci. USA *109*, 8576–8581.

Ebrahim, S., Fujita, T., Millis, B.A., Kozin, E., Ma, X., Kawamoto, S., Baird, M.A., Davidson, M., Yonemura, S., Hisa, Y., et al. (2013). NMII forms a contractile transcellular sarcomeric network to regulate apical cell junctions and tissue geometry. Curr. Biol. *23*, 731–736.

Fanning, A.S., Van Itallie, C.M., and Anderson, J.M. (2012). Zonula occludens-1 and -2 regulate apical cell structure and the zonula adherens cytoskeleton in polarized epithelia. Mol. Biol. Cell *23*, 577–590.

Goode, B.L., and Eck, M.J. (2007). Mechanism and function of formins in the control of actin assembly. Annu. Rev. Biochem. *76*, 593–627.

Grashoff, C., Hoffman, B.D., Brenner, M.D., Zhou, R., Parsons, M., Yang, M.T., McLean, M.A., Sligar, S.G., Chen, C.S., Ha, T., and Schwartz, M.A. (2010). Measuring mechanical tension across vinculin reveals regulation of focal adhesion dynamics. Nature *466*, 263–266.

Grikscheit, K., Frank, T., Wang, Y., and Grosse, R. (2015). Junctional actin assembly is mediated by Formin-like 2 downstream of Rac1. J. Cell Biol. *209*, 367–376.

Gumbiner, B., Stevenson, B., and Grimaldi, A. (1988). The role of the cell adhesion molecule uvomorulin in the formation and maintenance of the epithelial junctional complex. J. Cell Biol. *107*, 1575–1587.

Haviv, L., Gillo, D., Backouche, F., and Bernheim-Groswasser, A. (2008). A cytoskeletal demolition worker: Myosin II acts as an actin depolymerization agent. J. Mol. Biol. *375*, 325–330.

Homem, C.C., and Peifer, M. (2008). Diaphanous regulates myosin and adherens junctions to control cell contractility and protrusive behavior during morphogenesis. Development *135*, 1005–1018.

Jodoin, J.N., Coravos, J.S., Chanet, S., Vasquez, C.G., Tworoger, M., Kingston, E.R., Perkins, L.A., Perrimon, N., and Martin, A.C. (2015). Stable Force Balance between Epithelial Cells Arises from F-Actin Turnover. Dev. Cell *35*, 685–697.

Kannan, N., and Tang, V.W. (2015). Synaptopodin couples epithelial contractility to α-actinin-4-dependent junction maturation. J. Cell Biol. *211*, 407–434.

Kobielak, A., Pasolli, H.A., and Fuchs, E. (2004). Mammalian formin-1 participates in adherens junctions and polymerization of linear actin cables. Nat. Cell Biol. *6*, 21–30.

Kovacs, E.M., Verma, S., Ali, R.G., Ratheesh, A., Hamilton, N.A., Akhmanova, A., and Yap, A.S. (2011). N-WASP regulates the epithelial junctional actin cytoskeleton through a non-canonical post-nucleation pathway. Nat. Cell Biol. *13*, 934–943.

Lecuit, T., and Yap, A.S. (2015). E-cadherin junctions as active mechanical integrators in tissue dynamics. Nat. Cell Biol. *17*, 533–539.

Leerberg, J.M., Gomez, G.A., Verma, S., Moussa, E.J., Wu, S.K., Priya, R., Hoffman, B.D., Grashoff, C., Schwartz, M.A., and Yap, A.S. (2014). Tension-sensitive actin assembly supports contractility at the epithelial zonula adherens. Curr. Biol. *24*, 1689–1699.

Li, F., and Higgs, H.N. (2003). The mouse Formin mDia1 is a potent actin nucleation factor regulated by autoinhibition. Curr. Biol. *13*, 1335–1340.

Madara, J.L. (1987). Intestinal absorptive cell tight junctions are linked to the cytoskeleton. Am. J. Physiol. *253*, C171–C175.

Marchiando, A.M., Graham, W.V., and Turner, J.R. (2010). Epithelial barriers in homeostasis and disease. Annu. Rev. Pathol. *5*, 119–144.

Martin, A.C., and Goldstein, B. (2014). Apical constriction: Themes and variations on a cellular mechanism driving morphogenesis. Development *141*, 1987–1998.

Mason, F.M., Tworoger, M., and Martin, A.C. (2013). Apical domain polarization localizes actin-myosin activity to drive ratchet-like apical constriction. Nat. Cell Biol. *15*, 926–936.

Mason, F.M., Xie, S., Vasquez, C.G., Tworoger, M., and Martin, A.C. (2016). RhoA GTPase inhibition organizes contraction during epithelial morphogenesis. J. Cell Biol. *214*, 603–617.

Meng, W., Mushika, Y., Ichii, T., and Takeichi, M. (2008). Anchorage of microtubule minus ends to adherens junctions regulates epithelial cell-cell contacts. Cell *135*, 948–959.

Michael, M., Meiring, J.C., Acharya, B.R., Matthews, D.R., Verma, S., Han, S.P., Hill, M.M., Parton, R.G., Gomez, G.A., and Yap, A.S. (2016). Coronin 1B Reorganizes the Architecture of F-Actin Networks for Contractility at Steady-State and Apoptotic Adherens Junctions. Dev. Cell *37*, 58–71.

Murrell, M., Oakes, P.W., Lenz, M., and Gardel, M.L. (2015). Forcing cells into shape: The mechanics of actomyosin contractility. Nat. Rev. Mol. Cell Biol. *16*, 486–498.

Nusrat, A., Giry, M., Turner, J.R., Colgan, S.P., Parkos, C.A., Carnes, D., Lemichez, E., Boquet, P., and Madara, J.L. (1995). Rho protein regulates tight junctions and perijunctional actin organization in polarized epithelia. Proc. Natl. Acad. Sci. USA *92*, 10629–10633.

Ohsugi, M., Larue, L., Schwarz, H., and Kemler, R. (1997). Cell-junctional and cytoskeletal organization in mouse blastocysts lacking E-cadherin. Dev. Biol. *185*, 261–271.

Peng, J., Wallar, B.J., Flanders, A., Swiatek, P.J., and Alberts, A.S. (2003). Disruption of the Diaphanous-related formin Drf1 gene encoding mDia1 reveals a role for Drf3 as an effector for Cdc42. Curr. Biol. *13*, 534–545.

Priya, R., and Yap, A.S. (2015). Active tension: The role of cadherin adhesion and signaling in generating junctional contractility. Curr. Top. Dev. Biol. *112*, 65–102.

Priya, R., Yap, A.S., and Gomez, G.A. (2013). E-cadherin supports steady-state Rho signaling at the epithelial zonula adherens. Differentiation *86*, 133–140.

Priya, R., Gomez, G.A., Budnar, S., Verma, S., Cox, H.L., Hamilton, N.A., and Yap, A.S. (2015). Feedback regulation through myosin II confers robustness on RhoA signalling at E-cadherin junctions. Nat. Cell Biol. *17*, 1282–1293.

Rao, M.V., and Zaidel-Bar, R. (2016). Formin-mediated actin polymerization at cell-cell junctions stabilizes E-cadherin and maintains monolayer integrity during wound repair. Mol. Biol. Cell *27*, 2844–2856.

Ratheesh, A., Gomez, G.A., Priya, R., Verma, S., Kovacs, E.M., Jiang, K., Brown, N.H., Akhmanova, A., Stehbens, S.J., and Yap, A.S. (2012). Central-spindlin and α-catenin regulate Rho signalling at the epithelial zonula adherens. Nat. Cell Biol. *14*, 818–828.

Reymann, A.C., Boujemaa-Paterski, R., Martiel, J.L., Guérin, C., Cao, W., Chin, H.F., De La Cruz, E.M., Théry, M., and Blanchoin, L. (2012). Actin network architecture can determine myosin motor activity. Science *336*, 1310–1314.

Rizvi, S.A., Neidt, E.M., Cui, J., Feiger, Z., Skau, C.T., Gardel, M.L., Kozmin, S.A., and Kovar, D.R. (2009). Identification and characterization of a small molecule inhibitor of formin-mediated actin assembly. Chem. Biol. *16*, 1158–1168.

Shapiro, L., and Weis, W.I. (2009). Structure and biochemistry of cadherins and catenins. Cold Spring Harb. Perspect. Biol. *1*, a003053.

Shen, L., Weber, C.R., and Turner, J.R. (2008). The tight junction protein complex undergoes rapid and continuous molecular remodeling at steady state. J. Cell Biol. *181*, 683–695.

Smutny, M., Cox, H.L., Leerberg, J.M., Kovacs, E.M., Conti, M.A., Ferguson, C., Hamilton, N.A., Parton, R.G., Adelstein, R.S., and Yap, A.S. (2010). Myosin II isoforms identify distinct functional modules that support integrity of the epithelial zonula adherens. Nat. Cell Biol. *12*, 696–702.

Takeichi, M. (2014). Dynamic contacts: Rearranging adherens junctions to drive epithelial remodelling. Nat. Rev. Mol. Cell Biol. *15*, 397–410.

Tang, V.W., and Brieher, W.M. (2012). α-Actinin-4/FSGS1 is required for Arp2/3-dependent actin assembly at the adherens junction. J. Cell Biol. *196*, 115–130.

Tunggal, J.A., Helfrich, I., Schmitz, A., Schwarz, H., Günzel, D., Fromm, M., Kemler, R., Krieg, T., and Niessen, C.M. (2005). E-cadherin is essential for in vivo epidermal barrier function by regulating tight junctions. EMBO J. *24*, 1146–1156.

Turner, J.R., Rill, B.K., Carlson, S.L., Carnes, D., Kerner, R., Mrsny, R.J., and Madara, J.L. (1997). Physiological regulation of epithelial tight junctions is associated with myosin light-chain phosphorylation. Am. J. Physiol. *273*, C1378–C1385.

Verma, S., Han, S.P., Michael, M., Gomez, G.A., Yang, Z., Teasdale, R.D., Ratheesh, A., Kovacs, E.M., Ali, R.G., and Yap, A.S. (2012). A WAVE2-Arp2/3 actin nucleator apparatus supports junctional tension at the epithelial zonula adherens. Mol. Biol. Cell *23*, 4601–4610.

Wheelock, M.J., and Jensen, P.J. (1992). Regulation of keratinocyte intercellular junction organization and epidermal morphogenesis by E-cadherin. J. Cell Biol. *117*, 415–425.

Wu, S.K., Gomez, G.A., Michael, M., Verma, S., Cox, H.L., Lefevre, J.G., Parton, R.G., Hamilton, N.A., Neufeld, Z., and Yap, A.S. (2014). Cortical F-actin stabilization generates apical-lateral patterns of junctional contractility that integrate cells into epithelia. Nat. Cell Biol. *16*, 167–178.

Yamada, S., Pokutta, S., Drees, F., Weis, W.I., and Nelson, W.J. (2005). Deconstructing the cadherin-catenin-actin complex. Cell *123*, 889–901.

Yao, M., Qiu, W., Liu, R., Efremov, A.K., Cong, P., Seddiki, R., Payre, M., Lim, C.T., Ladoux, B., Mège, R.M., and Yan, J. (2014). Force-dependent conformational switch of α-catenin controls vinculin binding. Nat. Commun. *5*, 4525.

Yonemura, S., Wada, Y., Watanabe, T., Nagafuchi, A., and Shibata, M. (2010). alpha-Catenin as a tension transducer that induces adherens junction development. Nat. Cell Biol. *12*, 533–542.